

# ChemComm

Chemical Communications

rsc.li/chemcomm



ISSN 1359-7345

**COMMUNICATION**

Jian-Ji Zhong, Xiao-Chun Huang *et al.*  
Building a cobaloxime-based metal–organic framework for  
photocatalytic aerobic oxidation of arylboronic acids to  
phenols


 Cite this: *Chem. Commun.*, 2023, 59, 2239

 Received 21st December 2022,  
Accepted 17th January 2023

DOI: 10.1039/d2cc06945h

rsc.li/chemcomm

## Building a cobaloxime-based metal–organic framework for photocatalytic aerobic oxidation of arylboronic acids to phenols†

 Yonghong Xiao,<sup>†</sup> Can-Ming Zhu,<sup>‡</sup> Rong-Bin Liang,<sup>a</sup> Yong-Liang Huang,<sup>†</sup> Chun-Hua Hai,<sup>a</sup> Jian-Rui Chen,<sup>a</sup> Mian Li,<sup>†</sup> Jian-Ji Zhong<sup>†</sup> and Xiao-Chun Huang<sup>†</sup>

Herein, the design and synthesis of an unprecedented cobaloxime-based zirconium metal–organic framework (Zr-TCPCo) with an she net is reported. This heterogeneous material as a photocatalyst exhibits excellent catalytic activity for aerobic oxidation of arylboronic acids to phenols. Recycling experiments demonstrate the stability and reusability of Zr-TCPCo as a robust catalyst.

Metal–organic frameworks (MOFs) play an important role in gas adsorption, biomedicine, catalysis, sensing, and other fields<sup>1</sup> after decades of development. In particular, owing to the easily modified porous structure of MOFs, photocatalysts such as atomic clusters, molecular-based photosensitizers, *etc.* can be dispersed in MOFs by loading or covalently/coordinate grafting and so on.<sup>2</sup> For some photocatalysts, the aggregation problem that leads to weakening of the light absorption capacity, and thus the reduction of the catalytic efficiency, can be alleviated under the protection of MOFs.<sup>3</sup> However, the reported hetero-assembled catalysts still face some problems such as the recovery of the catalysts, uncertainty of catalytic sites, low catalyst utilization, *etc.*, resulting in low catalytic efficiency and unclear catalytic mechanism. Due to the diverse modifiability of the ligands and metal nodes of the MOF itself, as well as the atomically precise dispersion of photocatalysts in the structures, which would contribute to the study of the mechanism, a more straightforward solution is to directly build MOFs as catalysts, such as the previously reported<sup>4</sup>

porphyrin-, carbazole-, and benzothiadiazole-based MOF materials. Among the numerous catalysts, cobaloxime complexes, initially developed as a mimic of vitamin B<sub>12</sub>, have been demonstrated to be a class of efficient molecular catalysts<sup>5</sup> for hydrogen evolution or organic transformations; in particular, the elegant combination of cobaloximes with photosensitizers was shown to be a powerful catalytic tool for cross-coupling reactions,<sup>6</sup> and therefore has received much attention in the past decade. Although beautiful chemistry based on molecular cobaloxime catalysts has been achieved, in contrast, the research for cobaloxime-based heterogeneous materials has to date been rarely explored. Hence, constructing a cobaloxime-based MOF material and exploring the catalytic activity will be appealing. In this context, we try to design an example of a cobaloxime-based MOF for photocatalytic reaction. Herein, we report the successful preparation of an unprecedented cobaloxime-based zirconium MOF (Zr-TCPCo). This easily prepared Zr-TCPCo as a photocatalyst was found to be efficient for catalytic oxidation of arylboronic acids to phenols under visible light. Recycling experiments demonstrated the stability and reusability of Zr-TCPCo as a robust photocatalyst.

The reticular construction of atomically-precise dispersed photocatalysts allows topological design<sup>7</sup> of the nanoscale spatial arrangement of the catalyst, as well as modulation of the micro-/meso-pore size and shape selectivity of the substrate transport. We selected the Zr-MOF platform because the Zr<sub>6</sub> cluster can be connected into networks with different coordination numbers varying from 4 to 12, which is closely related to the ligand conformation and connection mode as well as the synthetic conditions (*e.g.* solvent, temperature, modulator, reactant ratio, *etc.*).<sup>8</sup> As for a tetratopic (4-c) ligand that can immobilize a cobaloxime core, several possible minimal-transitivity nets can be constructed (Scheme S1, ESI<sup>†</sup>), such as (4,12)-c **ftw/shp**, (4,8)-c **csq/scu/sqc**, and (4,6)-c **she**.<sup>9</sup> With the aim to obtain a hierarchical porous framework, we chose the **she** topology (**s** for square; **he** for hexagon),<sup>10</sup> which contains a planar hexagonal 6-c node that can be achieved through partial

<sup>a</sup> Department of Chemistry and Key Laboratory for Preparation and Application of Ordered Structural Materials of Guangdong Province, Shantou University, Guangdong 515063, China. E-mail: jjzhong@stu.edu.cn, xchuang@stu.edu.cn

<sup>b</sup> Chemistry and Chemical Engineering Guangdong Laboratory, Shantou 515031, China

<sup>c</sup> Department of Medicinal Chemistry, Shantou University Medical College, Shantou, Guangdong 515041, China

† Electronic supplementary information (ESI) available. CCDC 2222381 and 2222429. For ESI and crystallographic data in CIF or other electronic format see DOI: <https://doi.org/10.1039/d2cc06945h>

‡ The two authors contributed equally to this work.

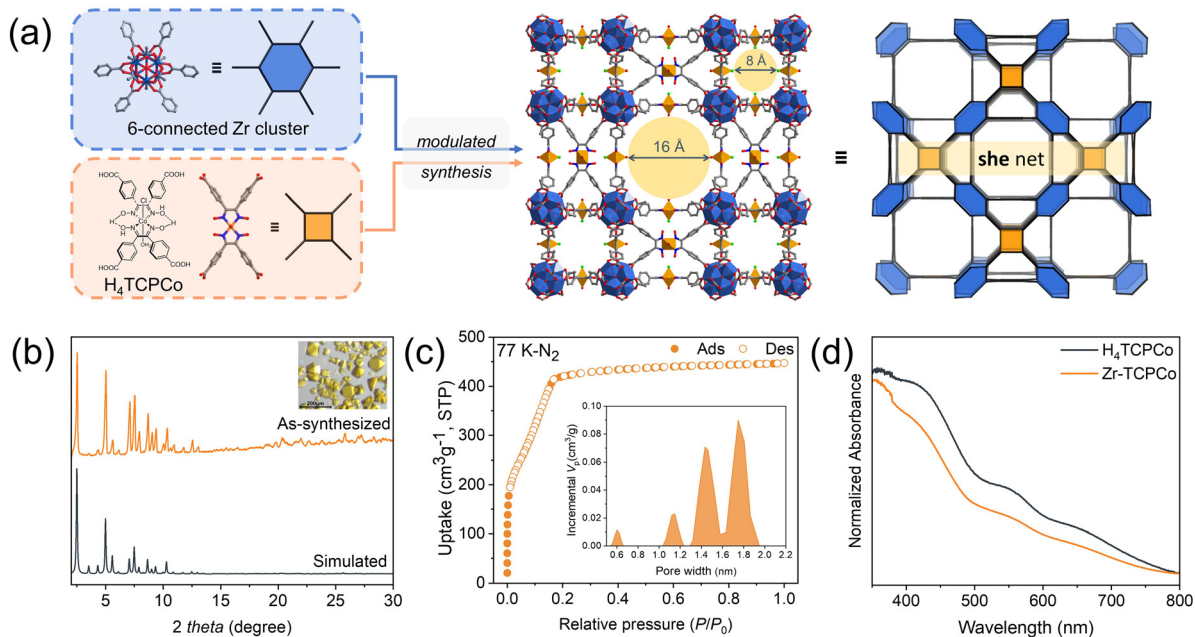


**Fig. 1** (a) Schematic illustration of the design and synthesis of Zr-TCPCo with a **she** net; (b) PXRD patterns of Zr-TCPCo; inset: Optical micrograph of Zr-TCPCo; (c) 77 K N<sub>2</sub> adsorption test of Zr-TCPCo; inset: diagram of incremental pore volume vs. pore width; (d) UV-vis spectra of Zr-TCPCo and the molecular cobaloxime H<sub>4</sub>TCPCo.

substitution of the full 12-c Zr<sub>6</sub> cluster by monocarboxylate modulators (e.g. acetate). It should be noted that there are two other edge-transitive (4,6)-c nets, **nts** and **cyb**, for linking squares and hexagons,<sup>11</sup> but they require parallel squares in close proximity, and so are not suitable for the cobaloxime moiety with axially coordinated molecules.

To verify our hypothesis, as shown in Fig. 1a, we formulated the reagents, containing zirconium salt and a rigid tetracarboxylate cobaloxime complex (H<sub>4</sub>TCPCo, Fig. 1a),<sup>12</sup> with 100 equivalent of acetic acid relative to H<sub>4</sub>TCPCo (details of the synthesis and characterization are given in the ESI†). To our delight, an unprecedented 3D structure (Zr-TCPCo) crystallized in the cubic space group *Pm3m*, yielding two types of channels (0.8 nm and 1.6 nm, Fig. 1c) with walls formed by cobaloximes,<sup>13</sup> which could facilitate the interaction of the substrate with the catalyst (Fig. 1a).

Note that even when the synthesis was scaled-up to 10-fold or 20-fold, it was confirmed by PXRD characterization that Zr-TCPCo was all in pure phase (Fig. 1b and Fig. S1, S2, ESI†). SEM and EDS mapping further revealed the fact that cobaloxime is evenly distributed in such truncated cubiform crystals (Fig. S3 and S4, ESI†). Considering that the redox property of cobaloxime may be affected under solvothermal conditions like other transition metals with variable valence,<sup>14</sup> an XPS test was conducted, and the results showed sharp peaks at 780 eV and 795 eV, indicating the trivalent nature of cobalt (Fig. S5, ESI†). Besides, Zr-TCPCo also showed the presence of micropores, which was indicated by the type I curve from the 77 K N<sub>2</sub> adsorption isotherm (Fig. 1c). Along with a maximum adsorption capacity of 447 cm<sup>3</sup> g<sup>-1</sup> and a BET surface area (1061 m<sup>2</sup> g<sup>-1</sup>), Zr-TCPCo exhibits the advantage of effective mass transfer in the heterogeneous catalytic process. In

addition, stability is a key factor worth considering for a catalyst.<sup>15</sup> Herein, Zr-TCPCo showed general stability towards most of the organic solvents (Fig. S10, ESI†) and pH stability (pH 1 to 12, Fig. S11, ESI†), as well as a significant thermal stability (up to 250 °C, Fig. S7–S9, ESI†), which provided a basis for its potential application. Compared to the materials that commonly need to be stored either in an inert atmosphere or at low temperature, Zr-TCPCo was found to be stable both in air and in water under ambient conditions (Fig. S12, ESI†), which is beneficial for long-term storage and usage of this material. Further investigation of the optical properties of Zr-TCPCo suggested a good visible-light absorbance (Fig. 1d) and a p-type semiconductor nature with a band gap of ~2.7 eV (Fig. S14 and S15, ESI†), which provided the possibility for its potential application in photocatalysis.

Photocatalytic oxidation of arylboronic acids has emerged as a powerful tool for the synthesis of phenols,<sup>16</sup> which widely exist in bioactive molecules and are used as intermediates in synthetic chemistry. With the cobaloxime-based MOF material in hand, we next explored the photocatalytic activity by using Zr-TCPCo as a sole photocatalyst and phenylboronic acid (**a1**) as a test substrate. To our delight, in the presence of a catalytic amount of Zr-TCPCo (3.0 mg) as a photocatalyst with excess triethylamine (Et<sub>3</sub>N) under a dioxygen (O<sub>2</sub>) atmosphere, a 0.2 mmol scale reaction proceeded smoothly to give the desired phenol **b1** in 91% yield at room temperature by 450 nm LED irradiation for 12 h (Table 1, entry 1). The solvent test revealed that several commonly used organic solvents showed comparable reaction efficiency (Table 1, entries 2–5). However, considering the convenience of catalyst recycling, dichloroethane (DCE) was the best choice. Compared with the case of a molecular

Table 1 Optimization of the reaction conditions<sup>a</sup>

Entry	Variation from the standard conditions	<b>b1</b> <sup>b</sup> (%)
1	None	91
2	Ethyl acetate instead of DCE	72
3	Acetone instead of DCE	89
4	Acetonitrile instead of DCE	88
5	Ethanol instead of DCE	90
6	H <sub>4</sub> TCPCo instead of Zr-TCPCo	66
7	Under air atmosphere	46(78) <sup>c</sup>
8	Under argon atmosphere	0
9	In dark	0
10	Without Zr-TCPCo	0
11	Without Et <sub>3</sub> N	0

<sup>a</sup> Reaction conditions: **a1** (0.2 mmol), Zr-TCPCo (3.0 mg), Et<sub>3</sub>N (2.0 equiv.), DCE (2 mL), 450 nm LED irradiation for 12 h at r.t. under O<sub>2</sub> atmosphere. <sup>b</sup> Isolated yields. <sup>c</sup> 24 h irradiation.

cobaloxime complex (H<sub>4</sub>TCPCo, 3.0 mg) as a photocatalyst, Zr-TCPCo obviously increased the efficiency (Table 1, entry 6). The O<sub>2</sub> atmosphere was essential to the reaction. If the reaction was carried out in an air atmosphere, a sharply decreased yield of 46% was obtained, yet prolonging the reaction time to 24 h could increase the yield to 78% (Table 1, entry 7). No desired product was detected under an argon atmosphere (Table 1, entry 8). Further control experiments revealed that light, Zr-TCPCo and Et<sub>3</sub>N were essential parameters to the reaction, and in their absence, no desired transformation was observed (Table 1, entries 8–11).

With the optimal conditions established, we proceeded to investigate the generality of Zr-TCPCo as a heterogeneous photocatalyst for this transformation. As shown in Table 2, when a broad range of phenylboronic acids bearing electron-withdrawing or electron-donating groups at different positions on the phenyl ring were attempted, the corresponding phenols were obtained in good to excellent yields (**b1**–**b18**). To demonstrate the practical synthesis using this heterogeneous catalyst, a 10 mmol scale reaction of **a1** was conducted, and the desired product **b1** was obtained in 76% yield with a prolonged reaction time (36 h). Polycyclic aromatic boronic acids such as 2-naphthaleneboronic acid (**b19**), 1-pyrenylboronic acid (**b20**) and 9,9'-spirobi[9*H*-fluorene]-2-boronic acid (**b21**) were also compatible with the reaction, giving the yields of 75%, 59% and 78%, respectively. Note that the structure of **b21** has been confirmed by single-crystal X-ray diffraction analysis<sup>17</sup> (see Section 16 in the ESI<sup>†</sup>). Furthermore, the heteroarylboronic acids or heterocyclic-fused phenylboronic acids were also effective substrates in this reaction with good yields (**b22**–**b26**).

Compared with homogeneous catalysts, heterogeneous catalysts have the advantage of being recyclable. To investigate the recyclability of Zr-TCPCo in the reaction, the reaction using **a1** as the substrate was selected for the recycling experiments. After each run, the catalyst Zr-TCPCo could be easily separated and recovered by centrifugation and directly used for the next cycle under the same procedure. As shown in Fig. 2, after being

Table 2 Substrate scope of arylboronic acids<sup>ab</sup>

<b>b1</b> , R = H, 91% (0.714 g, 76%)	<b>b6</b> , R = OH, 86%	<b>b12</b> , 74%	<b>b13</b> , 81%
<b>b2</b> , R = F, 60%	<b>b7</b> , R = <i>n</i> -pentyl, 75%	<b>b16</b> , 97%	<b>b17</b> , 65%
<b>b3</b> , R = Cl, 77%	<b>b8</b> , R = OPh, 88%	<b>b19</b> , 75%	<b>b20</b> , 59%
<b>b4</b> , R = Br, 74%	<b>b9</b> , R = OCH <sub>2</sub> Ph, 70%	<b>b21</b> , 78%	<b>b22</b> , 90%
<b>b5</b> , R = CN, 53%	<b>b10</b> , R = NPPh <sub>2</sub> , 77%	<b>b23</b> , 73%	<b>b24</b> , 61%
	<b>b11</b> , R = Cz = <i>N</i> -Carbazolyl, 95%	<b>b25</b> , 70%	<b>b26</b> , 59%

<sup>a</sup> Reaction conditions: **a** (0.2 mmol), Zr-TCPCo (3.0 mg), Et<sub>3</sub>N (2.0 equiv.), DCE (2 mL), 450 nm LEDs irradiation for 12 h at r.t. under O<sub>2</sub> atmosphere. <sup>b</sup> Isolated yields.

reused ten times, no significant loss of catalytic activity was observed. Interestingly, even after the Zr-TCPCo recovered from the tenth experiment was exposed to air and stored for two weeks, it still exhibited a satisfactory efficiency (Fig. 2, column 11). However, a slight efficiency decrease was observed from the recycling experiments, which is probably attributed to the partial decrease of the crystallinity and the slightly reduced cobalt-valence (Fig. S5d, ESI<sup>†</sup>) of the recovered Zr-TCPCo. Nevertheless, SEM and EDS mapping showed an even distribution of elements (Fig. S4, ESI<sup>†</sup>) within the shredded Zr-TCPCo crystal after catalysis. The VB-XPS spectrum (Fig. S6, ESI<sup>†</sup>) remained the same after catalysis. The UV-Vis spectrum of the recovered Zr-TCPCo (Fig. S17, ESI<sup>†</sup>) showed a similar adsorption band compared with H<sub>4</sub>TCPCo. These observations indicated that the cobaloxime complex was retained within the recovered Zr-TCPCo structure, which ensured the efficient catalytic activity. Compared with previous reports<sup>Ac,d</sup> using other MOF

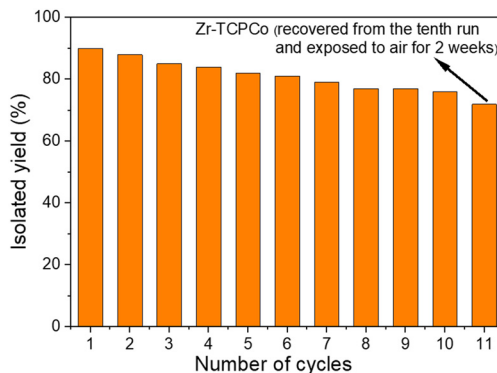


Fig. 2 Recyclability of the photocatalyst Zr-TCPCo.



Scheme 1 A plausible reaction pathway.

materials for this transformation, a broad scope of substrates was attempted, and less reaction time and more recycling cycles have been achieved. These above results demonstrated the stability and reusability of Zr-TCPCo as a robust catalyst.

Previous studies suggested that the superoxide radical anion ( $O_2^{\bullet-}$ ) is a key reactive intermediate in this transformation. Herein, the ideal band gap of Zr-TCPCo (2.7 eV) is believed to be capable of activating dioxygen to generate the superoxide radical anion by single electron transfer. Hence, a plausible reaction pathway was proposed, as illustrated in Scheme 1. The photo-excited Zr-TCPCo\* firstly reacts with dioxygen to generate  $O_2^{\bullet-}$ , which is further captured by arylboronic acid to furnish intermediate I-2. Then I-2 abstracts a hydrogen atom from I-1 to form intermediate I-3, followed by a rearrangement process to generate intermediate I-5. Finally, the subsequent hydrolysis of I-5 leads to the desired product.

In summary, we successfully designed and developed an easily-handled and operationally-simple method for the preparation of an unprecedented cobaloxime-based Zr-MOF with an **she** topology. Zr-TCPCo as a heterogeneous photo-catalyst showed excellent catalytic activity for the aerobic oxidation of arylboronic acids to phenols under mild conditions. Recycling experiments demonstrated the stability and reusability of Zr-TCPCo as a robust catalyst. Further exploration of the cobaloxime-based MOF material for photocatalytic organic transformations is ongoing in our laboratory.

The authors gratefully acknowledge the financial support from the National Natural Science Foundation of China (22171177 and 22071142), the Chemistry and Chemical Engineering Guangdong Laboratory (1922003), the Guangdong Major Project of Basic and Applied Basic Research (2019B030302009), and Li Ka Shing Foundation Cross-Disciplinary Research Project (Grant No. 2020LKSFG09A and 2020LKSFG10A).

## Conflicts of interest

There are no conflicts to declare.

## Notes and references

1 (a) R. Freund, S. Canossa, S. M. Cohen, W. Yan, H. Deng, V. Guillerme, M. Eddaoudi, D. G. Madden, D. Fairen-Jimenez, H. Lyu, L. K. Macreadie,

- Z. Ji, Y. Zhang, B. Wang, F. Haase, C. Wöll, O. Zaremba, J. Andreato, S. Wuttke and C. S. Diercks, *Angew. Chem., Int. Ed.*, 2021, **60**, 23946–23974; (b) X. Deng, Z. Li and H. Garcia, *Chem. – Eur. J.*, 2017, **23**, 11189–11209; (c) A. Dhakshinamoorthy, Z. Li and H. Garcia, *Chem. Soc. Rev.*, 2018, **47**, 8134–8172; (d) M. Hao and Z. Li, *Sol. RRL*, 2021, **5**, 2000454.
- 2 (a) S. Dai, T. Kajiwara, M. Ikeda, I. Romero-Muñiz, G. Patriarche, A. E. Platero-Prats, A. Vimont, M. Daturi, A. Tissot, Q. Xu and C. Serre, *Angew. Chem., Int. Ed.*, 2022, **61**, e202211848; (b) R. Navarro Amador, M. Carboni and D. Meyer, *RSC Adv.*, 2017, **7**, 195–200; (c) Q. Wang, Q. Gao, A. M. Al-Enizi, A. Nafady and S. Ma, *Inorg. Chem. Front.*, 2020, **7**, 300–339; (d) H.-L. Zhou, J. Bai, X.-Y. Tian, Z.-W. Mo and X.-M. Chen, *Chin. J. Chem.*, 2021, **39**, 2718–2724; (e) X. Deng, Y. Qin, M. Hao and Z. Li, *Inorg. Chem.*, 2019, **58**, 16574–16580; (f) Y. Qin, M. Hao, D. Wang and Z. Li, *Dalton Trans.*, 2021, **50**, 13201–13215.
- 3 Z. Liang, C. Qu, D. Xia, R. Zou and Q. Xu, *Angew. Chem., Int. Ed.*, 2018, **57**, 9604–9633.
- 4 (a) D.-Y. Zheng, E.-X. Chen, C.-R. Ye and X.-C. Huang, *J. Mater. Chem. A*, 2019, **7**, 22084–22091; (b) T. Ma, K. Li, J. Hu, Y. Xin, J. Cao, J. He and Z. Xu, *Inorg. Chem.*, 2022, **61**, 14352–14360; (c) J.-K. Jin, K. Wu, X.-Y. Liu, G.-Q. Huang, Y.-L. Huang, D. Luo, M. Xie, Y. Zhao, W. Lu, X.-P. Zhou, J. He and D. Li, *J. Am. Chem. Soc.*, 2021, **143**, 21340–21349; (d) X. Yu and S. M. Cohen, *Chem. Commun.*, 2015, **51**, 9880–9883.
- 5 (a) J. L. Dempsey, B. S. Brunschwig, J. R. Winkler and H. B. Gray, *Acc. Chem. Res.*, 2009, **42**, 1995–2004; (b) T. Lazarides, T. McCormick, P. W. Du, G. G. Luo, B. Lindley and R. Eisenberg, *J. Am. Chem. Soc.*, 2009, **131**, 9192–9194; (c) B. Chen, L.-Z. Wu and C.-H. Tung, *Acc. Chem. Res.*, 2018, **51**, 2512–2523.
- 6 (a) Q.-Y. Meng, J.-J. Zhong, Q. Liu, X.-W. Gao, H.-H. Zhang, T. Lei, Z.-J. Li, K. Feng, B. Chen, C.-H. Tung and L.-Z. Wu, *J. Am. Chem. Soc.*, 2013, **135**, 19052–19055; (b) J.-J. Zhong, Q.-Y. Meng, B. Liu, X.-B. Li, X.-W. Gao, T. Lei, C.-J. Wu, Z.-J. Li, C.-H. Tung and L.-Z. Wu, *Org. Lett.*, 2014, **16**, 1988–1991; (c) G. Zhang, C. Liu, H. Yi, Q. Meng, C. Bian, H. Chen, J. X. Jian, L.-Z. Wu and A. Lei, *J. Am. Chem. Soc.*, 2015, **137**, 9273–9280; (d) Y.-W. Zheng, B. Chen, P. Ye, K. Feng, W. Wang, Q.-Y. Meng, L.-Z. Wu and C.-H. Tung, *J. Am. Chem. Soc.*, 2016, **138**, 10080–10083; (e) W.-Q. Liu, T. Lei, S. Zhou, X.-L. Yang, J. Li, B. Chen, J. Sivaguru, C.-H. Tung and L.-Z. Wu, *J. Am. Chem. Soc.*, 2019, **141**, 13941–13947; (f) H. Zhang, Q. Xiao, X.-K. Qi, X.-W. Gao, Q.-X. Tong and J.-J. Zhong, *Chem. Commun.*, 2020, **56**, 12530–12533; (g) Q. Xiao, H. Zhang, J.-H. Li, J.-X. Jian, Q.-X. Tong and J.-J. Zhong, *Org. Lett.*, 2021, **23**, 3604–3609; (h) H. Xu, H. Zhang, Q.-X. Tong and J.-J. Zhong, *Org. Biomol. Chem.*, 2021, **19**, 8227–8231.
- 7 (a) M. Li, D. Li, M. O’Keeffe and O. M. Yaghi, *Chem. Rev.*, 2014, **114**, 1343–1370; (b) Z. Chen, H. Jiang, M. Li, M. O’Keeffe and M. Eddaoudi, *Chem. Rev.*, 2020, **120**, 8039–8065.
- 8 Y. Bai, Y. Dou, L. H. Xie, W. Rutledge, J. R. Li and H. C. Zhou, *Chem. Soc. Rev.*, 2016, **45**, 2327–2367.
- 9 (a) J. Lyu, X. Zhang, K. I. Otake, X. Wang, P. Li, Z. Li, Z. Chen, Y. Zhang, M. C. Wasson, Y. Yang, P. Bai, X. Guo, T. Islamoglu and O. K. Farha, *Chem. Sci.*, 2019, **10**, 1186–1192; (b) Y. Chen, X. Zhang, M. R. Mian, F. A. Son, K. Zhang, R. Cao, Z. Chen, S. J. Lee, K. B. Idrees, T. A. Goetjen, J. Lyu, P. Li, Q. Xia, Z. Li, J. T. Hupp, T. Islamoglu, A. Napolitano, G. W. Peterson and O. K. Farha, *J. Am. Chem. Soc.*, 2020, **142**, 21428–21438.
- 10 Z.-J. Li, X. Wang, L. Zhu, Y. Ju, Z. Wang, Q. Zhao, Z.-H. Zhang, T. Duan, Y. Qian, J.-Q. Wang and J. Lin, *Inorg. Chem.*, 2022, **61**, 7467–7476.
- 11 M. Li, M. O’Keeffe, D. M. Proserpio and H.-F. Zhang, *Cryst. Growth Des.*, 2020, **20**, 4062–4068.
- 12 S. Roy, Z. Huang, A. Bhunia, A. Castner, A. K. Gupta, X. Zou and S. Ott, *J. Am. Chem. Soc.*, 2019, **141**, 15942–15950.
- 13 For detailed information, see the ESI† and CCDC 2222381.
- 14 (a) P. Schmieder, D. Denysenko, M. Grzywa, O. Magdysyuk and D. Volkmer, *Dalton Trans.*, 2016, **45**, 13853–13862; (b) Y. Xiao, M. Li, J.-R. Chen, X. Lian, Y.-L. Huang and X.-C. Huang, *Inorg. Chem. Front.*, 2022, **9**, 6124–6132.
- 15 M. Ding, X. Cai and H.-L. Jiang, *Chem. Sci.*, 2019, **10**, 10209–10230.
- 16 (a) Y. Q. Zou, J. R. Chen, X. P. Liu, L. Q. Lu, R. L. Davis, K. A. Jorgensen and W. J. Xiao, *Angew. Chem., Int. Ed.*, 2012, **51**, 784–788; (b) S. P. Pitre, C. D. McTiernan, H. Ismaili and J. C. Scaiano, *J. Am. Chem. Soc.*, 2013, **135**, 13286–13289; (c) W. R. Leow, J. Yu, B. Li, B. Hu, W. Li and X. Chen, *Angew. Chem., Int. Ed.*, 2018, **57**, 9780–9784.
- 17 For detailed information, see the ESI† and CCDC 2222429.